



OPEN

## Metformin and berberine synergistically improve NAFLD via the AMPK–SREBP1–FASN signaling pathway

Na Li<sup>1,3</sup>, Quan-wei Chen<sup>2,3</sup>, Xiao-long Gong<sup>1</sup>, Fang Liu<sup>1</sup>, Bin Zhang<sup>1</sup>, Qi-shen Wang<sup>1</sup>, Hao Zhang<sup>1</sup> & Jian-jun Han<sup>1</sup>✉

Nonalcoholic fatty liver disease (NAFLD) is a prevalent metabolic condition linked to dyslipidemia, insulin resistance, and persistent inflammation. Due to its complex pathogenesis, no approved pharmacological treatments currently exist. The research sought to explore the combined impact of metformin (Met) and berberine (BBR) on NAFLD, focusing on the AMPK–SREBP1–FASN pathway implicated in liver lipid regulation. The study design incorporated in both living organisms and laboratory conditions to examine how these interventions influenced NAFLD-associated metabolic abnormalities. The HFD-fed mice provided insight into systemic effects, while the OA/PA-stimulated HepG2 cells offered a controlled environment to investigate cellular mechanisms. By employing this dual approach, the researchers could thoroughly characterize the efficacy of Met, BBR, and their combination in mitigating metabolic disturbances. An Adenosine 5'-monophosphate (AMP)-activated protein kinase(AMPK) inhibitor was used in cellular experiments to verify the AMPK-dependent mechanism. Our findings highlight that compared to monotherapies, combination treatment significantly enhanced AMPK activation and inhibited sterol regulatory element-binding protein 1 (SREBP1) expression and that of its downstream target fatty acid synthase (FASN). In HepG2 cells, these effects were partially reversed by the AMPK inhibitor, confirming AMPK dependence. In vivo, the combined therapy effectively inhibited body weight gain, reduced visceral fat accumulation, improved insulin sensitivity, and attenuated hepatic steatosis and inflammation. The combination of metformin and berberine exerts synergistic effects in ameliorating NAFLD by activating AMPK, downregulating SREBP1 and FASN, and improving lipid metabolism. These findings provide evidence supporting a potentially effective multi-modal treatment approach for NAFLD.

**Keywords** NAFLD, Metformin, Berberine, AMPK signaling, Synergistic therapy

Currently, non-alcoholic fatty liver disease (NAFLD) stands as the most widespread chronic liver disorder worldwide. Its surge parallels the global uptick in metabolic syndrome, obesity, and type2 diabetes<sup>1</sup>. NAFLD isn't merely one static disorder—it's a spectrum that begins with harmless fat accumulation but can progressively worsen into nonalcoholic Steatohepatitis (NASH), significant fibrosis, full-blown cirrhosis, and ultimately hepatocellular carcinoma. The condition evolves through distinct phases, each carrying greater health risks than the last. The stakes are high, and the numbers keep climbing<sup>2</sup>. The incidence of NAFLD is driven by multiple factors. Among them, lipid metabolism disorders and insulin resistance constitute the metabolic basis, while oxidative stress and chronic low-grade inflammation further promote the disease process.

To date, no particular pharmaceutical treatments have been authorized as of yet to treat NAFLD, highlighting the critical demand for efficient and secure approaches<sup>3</sup>. A common antidiabetic medication, metformin (Met), improves insulin sensitivity and controls energy homeostasis mainly by stimulating the AMPK signaling cascade<sup>4,5</sup>. Berberine (BBR), an alkaloid isoquinoline sourced from *Coptis chinensis*, exhibits lipid-lowering, glucose-lowering, and anti-inflammatory properties, also in part via AMPK activation<sup>1,6</sup>. Nevertheless,

<sup>1</sup> Department of Interventional Radiology, Shandong Cancer Hospital and Institute Affiliated Shandong First Medical University and Shandong Academy of Medical Sciences, Jinan 250117, China No. 440, Jiyan Road. <sup>2</sup>Shandong Second Medical University, Weifang 261053, China. <sup>3</sup>These authors Chen contributed equally to this work: Na Li and Quan-wei Chen. ✉email: hanjianjun@sdfmu.edu.cn

preclinical and clinical research has suggested that either Met or BBR alone may have limited effectiveness in treating the intricate inflammatory and metabolic abnormalities linked to NAFLD.

As a result, combination therapies with synergistic mechanisms of action have attracted increasing attention as promising approaches for managing the multifaceted nature of NAFLD. Although previous studies have demonstrated that both Met and BBR exert beneficial metabolic effects via AMPK activation<sup>7,8</sup>, whether their combination provides superior therapeutic outcomes, and whether such benefits are mediated through the AMPK–SREBP1–FASN signaling axis, still needs to be completely explained.

This research investigated the metabolic impact of administering both Met and BBR by employing two experimental approaches: a rodent model for NAFLD resulting from a hyperlipidic diet, along with HepG2 cells treated with oleic and palmitic acids. Additionally, we examined the engagement of the AMPK–SREBP1–FASN signaling axis in mediating the combined therapeutic effects, aiming to provide mechanistic insights and experimental evidence supporting their co-administration as a novel strategy for NAFLD management.

## Results

### Metformin and Berberine therapy enhances obesity management and insulin responsiveness in rodents with diet-induced obesity

To evaluate the synergistic effects of Met and BBR co-treatment on obesity and insulin resistance in a NAFLD mouse model, an HFD-induced NAFLD model was established. Subsequently, mice were administered Met, BBR, or their combination for 12 weeks. Body weight tracking showed a notable rise in the HFD group, whereas treatment with Met, BBR, and particularly their combination resulted in varying degrees of weight reduction, with the combination group exhibiting a trend of reduction (Fig. 1c–d). Importantly, although food intake showed some weekly variation among groups (Fig. 1b), no statistically significant differences were observed overall indicating that the observed weight changes were not primarily driven by reduced caloric intake. Liver mass (Fig. 1e), hepatic-to-body mass ratio (Fig. 1f), and visceral fat mass (Fig. 1g) were markedly elevated in the HFD group, indicative of exacerbated hepatic lipid accumulation. Co-treatment significantly attenuated these elevations. Further metabolic assessments showed that fast glucose levels (GLU; Fig. 1h), pre-meal insulin levels (INS; Fig. 1i), and (HOMA-IR) were markedly elevated in the HFD group versus controls (Fig. 1j). Both Met and BBR interventions effectively mitigated these metabolic derangements. The combination treatment showed a greater improvement compared to Met alone ( $p < 0.05$ ), although the difference between the combination group and monotherapy group was not statistically significant. These findings suggest a synergistic effect of Met and BBR in alleviating obesity-associated metabolic dysfunctions, with combination therapy demonstrating superior efficacy over monotherapy.

### Metformin combined with Berberine alleviates hepatocyte steatosis and dyslipidemia

Livers from HFD-fed mice were enlarged and exhibited a dark reddish coloration, indicative of fatty liver. Treatment with Met or BBR alone partially ameliorated these morphological abnormalities. Notably, the combined treatment restored liver size and color to near-normal levels (Fig. 2a). Hepatocytes from HFD animals showed widespread lipid aggregation when stained with Oil Red O, which was alleviated by either treatment alone and further reduced in the combination group (Fig. 2b–c). Hepatic triglyceride (TG) and total cholesterol (TC) levels were significantly elevated in HFD mice but were markedly reduced by combination therapy (Fig. 2d–e). Serum lipid profiling indicated dyslipidemia in the HFD group, marked by high low-density lipoprotein cholesterol (LDL-C), TG, and TC, along with low high-density lipoprotein cholesterol (HDL-C) levels. Both Met and BBR partially corrected these abnormalities; however, combined treatment yielded the most pronounced improvements, with increased HDL-C, decreased LDL-C, TG, and TC levels (Fig. 2f–i). These results demonstrate that Met and BBR synergistically ameliorate hepatic steatosis and dyslipidemia more effectively than monotherapy, highlighting their combined therapeutic potential in NAFLD.

### Metformin combined with Berberine alleviates HFD-induced liver injury and inflammation by activating hepatic AMPK signaling and inhibiting the expression of SREBP1 and FASN

Hematoxylin-eosin (H&E) staining disclosed that the HFD group displayed a disturbance in liver tissue organization contrasting with the unaltered control group, characterized by extensive lipid droplet fusion within hepatocytes (indicated by yellow arrows), accompanied by significant inflammatory cell infiltration (black arrows) and Kupffer cell activation (red arrows). The NAFLD activity score (NAS) was significantly increased (Fig. 3a–b). Treatment with either Met or BBR partially alleviated these histopathological alterations. However, a significant reduction in NAS score was only observed in the combination group, as revealed by the individual scores for steatosis, inflammation, and ballooning. Notably, combined treatment produced the most pronounced improvement. The HFD group's serum alanine aminotransferase (ALT) and aspartate aminotransferase (AST) values were noticeably higher; both Met and BBR treatments significantly decreased these enzyme levels, with combination therapy demonstrating superior hepatoprotective effects (Fig. 3c). In HFD mice, there was a considerable rise in pro-inflammatory cytokines, such as tumor necrosis factor-alpha (TNF- $\alpha$ ), interleukin-1 beta (IL-1 $\beta$ ) and interleukin-6 (IL-6). Their expression was substantially suppressed following combined treatment (Fig. 3d–f), indicating effective attenuation of NAFLD-associated inflammation.

To investigate the underlying synergistic lipid-lowering mechanism, key proteins within the AMPK–SREBP1–FASN signaling pathway were analyzed. Phosphorylation of AMP-activated protein kinase (p-AMPK) was significantly reduced in the high-fat diet group, suggesting impaired AMPK function. Met treatment significantly restored p-AMPK levels, while BBR showed an increasing trend without reaching statistical significance. Combination therapy resulted in the most robust elevation of p-AMPK expression, and raised the p-AMPK/AMPK ratio ( $p < 0.05$ ) (Fig. 3g, i). Conversely, the HFD group exhibited elevated of sterol regulatory element-binding protein 1 (SREBP1) and fatty acid synthase (FASN) expression, which were significantly

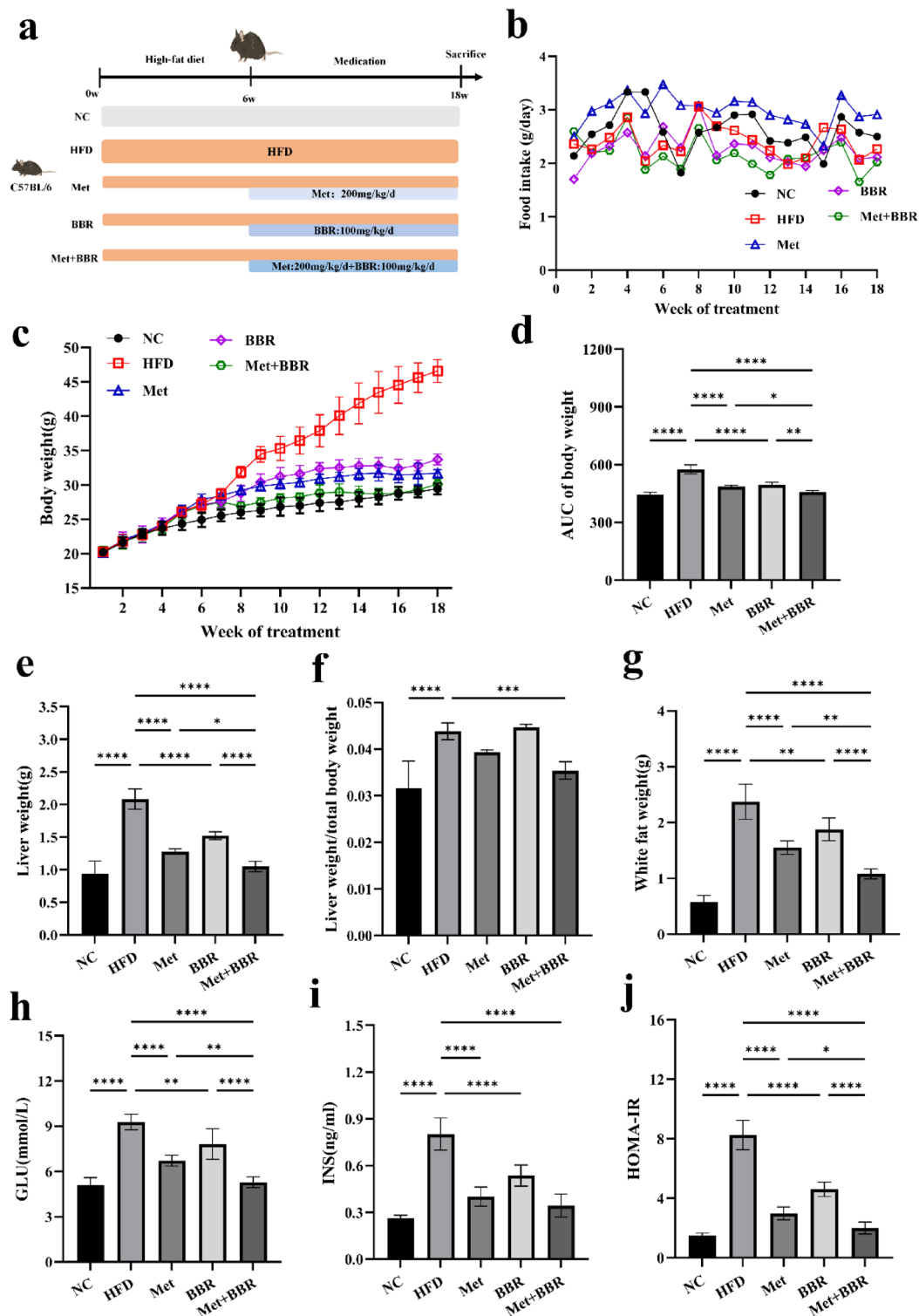


**Fig. 1.** Metformin combined with berberine intervention ameliorates high-fat diet (HFD)-induced obesity phenotype and insulin resistance in mice. **(a)** Schematic diagram illustrating the experimental procedure and grouping scheme; **(b)** Weekly food intake curves of mice in each group; **(c)** Longitudinal changes in body weight over 12 weeks of treatment; **(d)** Area under the curve (AUC) of body weight for each group; **(e)** Liver weight in each group; **(f)** Liver-to-body weight ratio (liver weight/body weight); **(g)** Visceral fat weight; **(h)** GLU; **(i)** INS; **(j)** HOMA-IR. Data are presented as mean  $\pm$  SEM ( $n=6$ ).  $^*p < 0.05$ ,  $^{**}p < 0.01$ ,  $^{***}p < 0.001$ ,  $^{****}p < 0.0001$ .

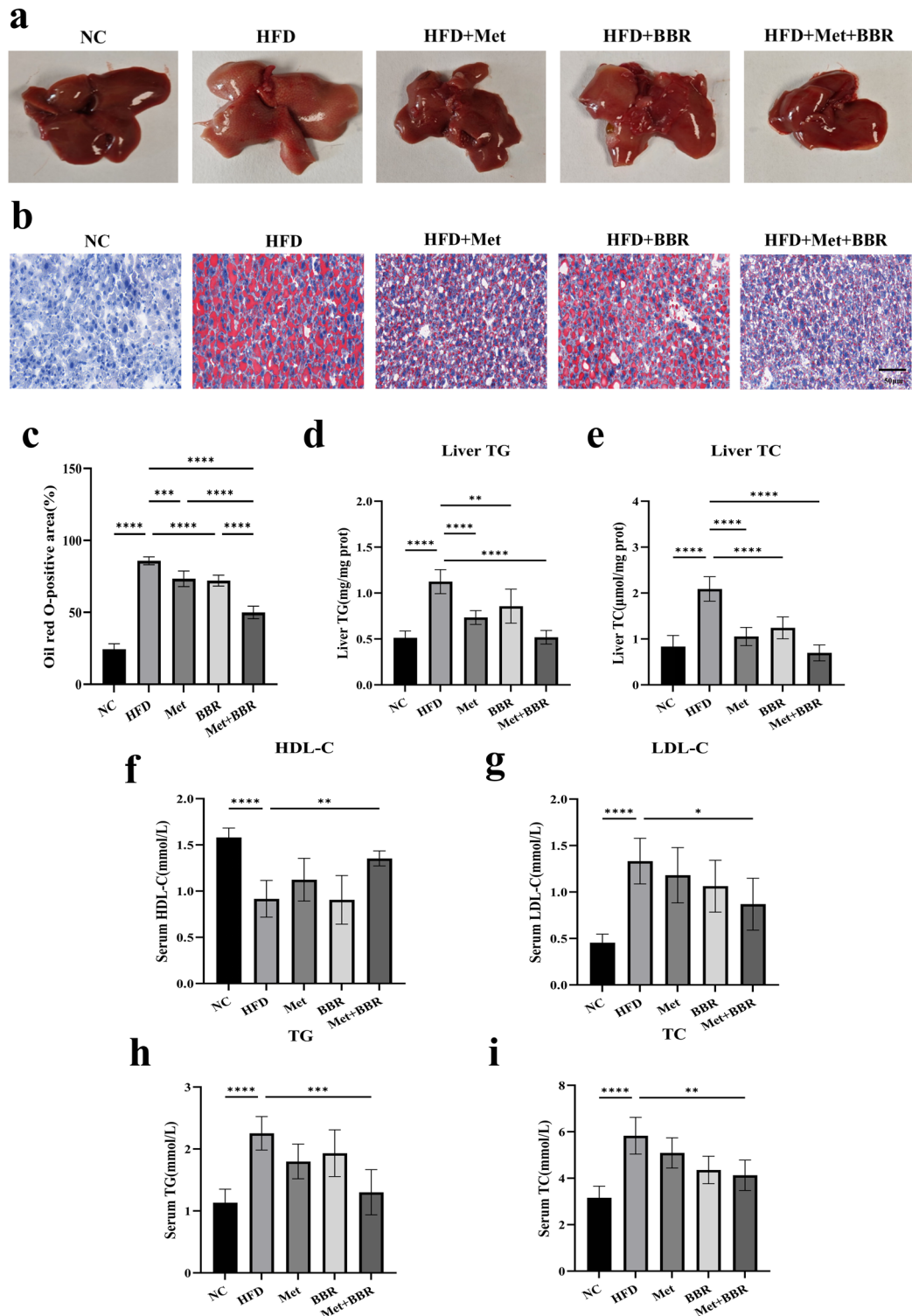


**Fig. 2.** Combined intervention with metformin and berberine effectively alleviates hepatic lipid accumulation and dyslipidemia induced by high-fat diet in mice. (a) Representative gross images of liver tissues from each group; (b) Oil Red O staining of liver sections (magnification = 20 $\times$ ; scale bar = 50  $\mu$ m) (c) Quantitative analysis of Oil Red O-positive areas; (d–e) Hepatic TG and TC levels; (f–i) Serum levels of HDL-C, LDL-C, TG, and TC. Data are presented as mean  $\pm$  SEM ( $n=6$ ). \* $p$  < 0.05, \*\* $p$  < 0.01, \*\*\* $p$  < 0.001, \*\*\*\* $p$  < 0.0001.

downregulated by the combination treatment, surpassing the effects of either monotherapy, (Fig. 3h, j–k). These results indicate that Met and BBR enhance liver lipid metabolism through AMPK pathway activation and inhibiting lipogenesis-related factors SREBP1 and FASN, thereby mitigating NAFLD pathology.

### Metformin combined with Berberine alleviates lipid accumulation and reduces triglyceride content in HepG2 cells

HepG2 cells were successfully used to establish an OA/PA-induced lipid accumulation model (Fig. 4a), as demonstrated by a significant increase in intracellular TG content and Oil Red O-positive staining areas (Fig. 4b–c). After selecting an appropriate concentration of high-fat culture medium (OA/PA = 200  $\mu$ M/100  $\mu$ M), cells were treated with various concentrations of metformin (Met) and berberine (BBR), followed by MTT assays. As described in the Methods section, the combination index (CI) was calculated (CI < 1) along with an  $IC_{50}$  value of 13.60  $\mu$ M, determining the previously optimal concentration<sup>9</sup>. Monotherapy with either agent significantly reduced intracellular lipid accumulation, with the combination treatment showing the most pronounced lipid-lowering effect. Subsequent Oil Red O staining quantification and TG assays further confirmed the synergistic lipid-lowering effect of the combination treatment (Fig. 4f–h).

### Metformin combined with Berberine synergistically activates AMPK and inhibits SREBP1 and FASN expression in HepG2 cells

In the OA/PA-induced HepG2 cell model, we further examined the expression levels of proteins involved in the AMPK–SREBP1–FASN signaling pathway. Western blot analysis revealed that the phosphorylation level of AMPK was elevated in the combination treatment group compared to the monotherapy groups (Fig. 5a, c), while the expression of SREBP1 and FASN was more markedly suppressed (Fig. 5b, d–e). These findings are consistent with the *in vivo* observations, suggesting that metformin and berberine exert a more pronounced lipid-lowering effect by synergistically activating the AMPK pathway and effectively inhibiting the expression of lipogenesis-related proteins.

### Metformin combined with Berberine exerts its effects by inhibiting lipid synthesis through the AMPK–SREBP1–FASN signaling pathway

In assessing the necessity of the AMPK pathway for the combined impact of Met and BBR, Compound C, an AMPK inhibitor, was employed. Results demonstrated that the significant reductions in cellular lipid accumulation (Fig. 6a–b) and TG content (Fig. 6c) observed in the combination treatment group were largely reversed following Compound C administration. Western blot analysis showed marked suppression of p-AMPK expression (Fig. 6d, f), followed by elevated FASN and SREBP1 protein levels (Fig. 6e, g–h). These findings indicate that the AMPK pathway is critical for in mediating the triglyceride-lowering effect of combined Met and BBR treatment in NAFLD.

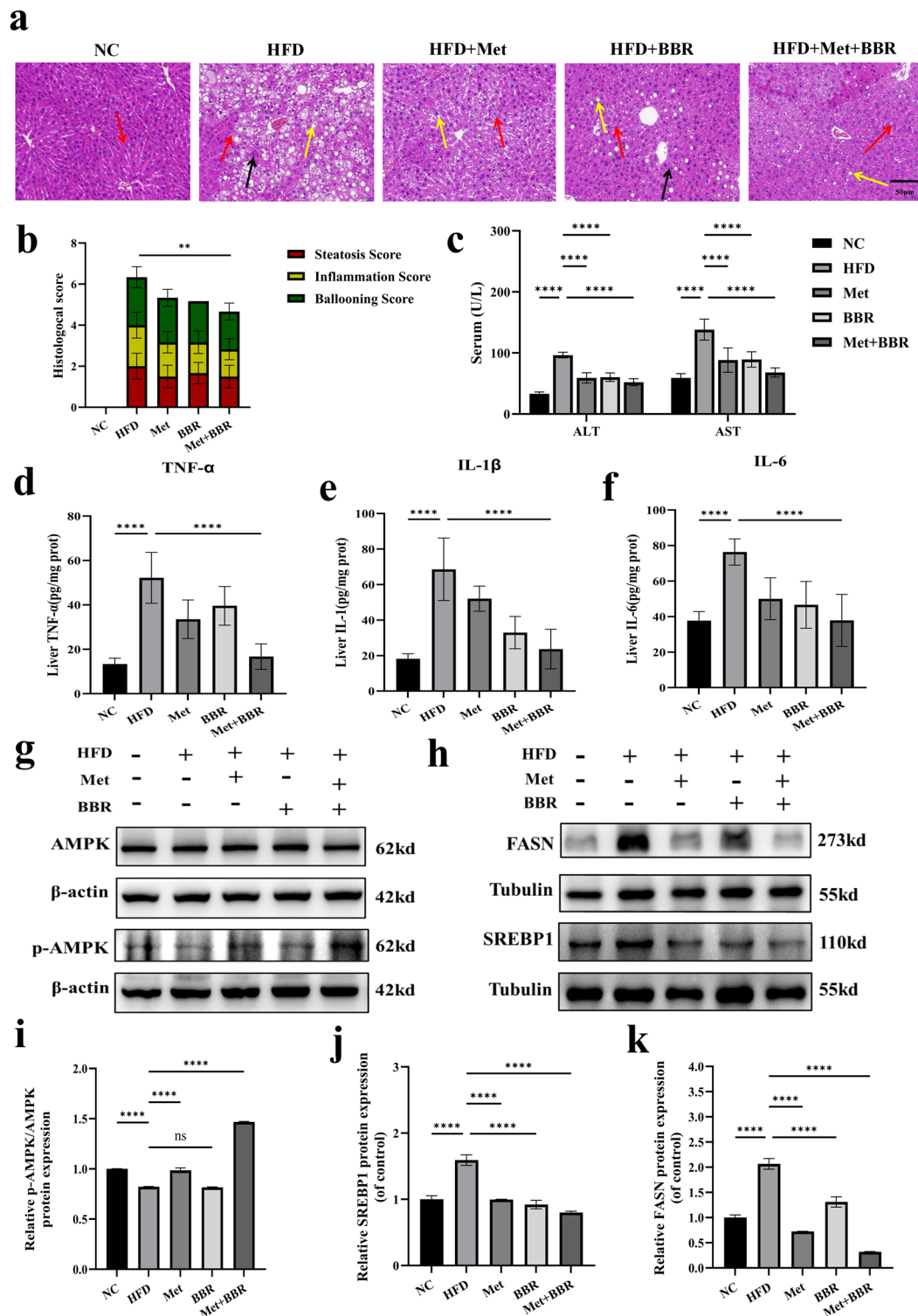
## Discussion

In animal and cellular models of NAFLD, the comprehensive evaluation of the metabolic impacts of Met and BBR treatments was conducted in this work. In mitigating HFD-induced hepatic steatosis, insulin resistance, weight gain, and liver inflammation, the combination therapy worked better than monotherapies, according to the results. Especially in animal experiment design, we employed a therapeutic model that better simulates clinical scenarios. NAFLD was first induced by six weeks of HFD feeding, followed by 12 weeks of drug administration starting at week 7. This post-diagnosis intervention paradigm more accurately reflects real-world clinical treatment, allowing for assessment of therapeutic reversal rather than prevention. These findings suggest that Met and BBR exert synergistic effects in ameliorating metabolic dysfunctions associated with NAFLD.

Our results demonstrated that although monotherapies with metformin (Met) or berberine (BBR) partially alleviated hepatic structural abnormalities and metabolic disturbances in NAFLD mice, neither treatment significantly improved the NAS score or its individual components (steatosis, inflammation, and ballooning). In contrast, the combination treatment led to significant improvements across all three histological parameters, suggesting a stronger synergistic effect on hepatic pathology. This divergence may be attributed to the complementary mechanisms of the two drugs: Met primarily activates the AMPK signaling pathway to inhibit lipogenesis and enhance fatty acid oxidation, thereby effectively reducing hepatic steatosis<sup>10</sup>, whereas BBR predominantly exerts anti-inflammatory and antioxidant effects, which help ameliorate inflammation and hepatocellular injury<sup>11,12</sup>.

Collectively, these findings suggest that Met and BBR synergistically target multiple pathological pathways, including lipid metabolism, inflammation, and insulin resistance, resulting in superior therapeutic efficacy compared to monotherapy. Natural compounds such as berberine, resveratrol, and quercetin, along with metabolic drugs like metformin, have demonstrated efficacy in ameliorating NAFLD via activation of AMPK and downregulation of SREBP1 and FASN<sup>13–17</sup>. Our findings expand this knowledge by showing that combination therapy achieves enhanced efficacy via overlapping and synergistic mechanisms, thereby supporting the rationale for multi-target pharmacological strategies.

Recent literature has underscored the importance of the AMPK–SREBP1–FASN pathway in NAFLD and other metabolic liver disorders<sup>18–20</sup>. Hepatic steatosis, insulin resistance, oxidative stress, and chronic inflammation are all exacerbated by the dysregulation of this system<sup>21</sup>. Consequently, it represents a promising target for novel therapeutic agents. This study focused on the AMPK–SREBP1–FASN axis due to its central role in NAFLD pathogenesis. To preserve hepatic lipid homeostasis, AMPK, a crucial cellular energy sensor, inhibits lipogenesis and encourages fatty acid oxidation<sup>22</sup>. SREBP1 regulates lipogenic gene expression, such as FASN<sup>23</sup>. AMPK inhibits SREBP1 activation and nuclear translocation, thereby reducing FASN expression and lipogenesis<sup>24</sup>. Our findings verified that this route is modulated by the combination of BBR and Met. The



observed reduction in FASN expression correlated with diminished lipid accumulation identified via Oil Red O staining, supporting a direct mechanistic link between pathway modulation and histological improvement. Further mechanistic studies showed that combination treatment significantly activated AMPK signaling in both liver tissues and HepG2 cells, accompanied by inhibition of SREBP1 and its downstream target FASN. This led to reduced lipogenesis and lipid accumulation in hepatocytes. Importantly, administration of an AMPK inhibitor partially reversed the suppression of SREBP1 and FASN, confirming that the lipid-lowering effect is dependent on AMPK activation. This is consistent with the research results of Li et al.<sup>24</sup>.

However, there are certain limitations in our experiment. Although our data confirm the key role of the AMPK-SREBP1-FASN pathway, other mechanisms, such as the mammalian target of rapamycin (mTOR)<sup>25,26</sup>, peroxisome proliferator activated receptor alpha (PPAR $\alpha$ )<sup>27</sup>, autophagy, and other inflammation-related pathways, not been adequately examined. Future studies need use immunoblotting and functional assays to assess fatty acid

**Fig. 3.** Metformin combined with berberine alleviates HFD-induced hepatic pathological injury and inflammation in mice, and inhibits key lipogenic protein expression via activation of the hepatic AMPK signaling pathway. **(a)** Representative H&E staining of liver tissues (magnification = 20 $\times$ ; scale bar = 50  $\mu$ m). Yellow arrows indicate fused lipid droplets; red arrows, Kupffer cells; black arrows, inflammatory cell infiltration; **(b)** Stacked bar chart of NAFLD activity scores including steatosis, inflammation, and ballooning components; **(c)** Serum ALT and AST levels; **(d-f)** Hepatic expression levels of TNF- $\alpha$ , interleukin-1 beta (IL-1 $\beta$ ), and IL-6; **(g)** Western blot bands of AMPK and phosphorylated AMPK (p-AMPK); **(h)** Western blot images of SREBP1 and FASN proteins; **(i-k)** Quantitative analyses of relative expression levels of p-AMPK/AMPK, SREBP1 and FASN. Data in panels a-g are presented as mean  $\pm$  SEM ( $n=6$  per group, animal experiments); data in panels h-l are presented as mean  $\pm$  SEM ( $n=3$  per group, representative of three independent experiments). To highlight the target bands, the images were cropped; the full-length gel/blot images are provided in the Supplementary Material. \*\* $p < 0.01$ , \*\*\* $p < 0.001$ , \*\*\*\* $p < 0.0001$ , ns: not significant.

oxidation and autophagic flux. Regarding AMPK activation, Met significantly increased p-AMPK expression, while BBR showed only a non-significant upward trend, indicating that its AMPK activation may be dose-dependent or context-specific. Nevertheless, BBR still exhibited strong anti-inflammatory effects in this study, possibly mediated by AMPK-independent mechanisms such as suppression of NF- $\kappa$ B and activation of Nrf2 signaling<sup>28</sup>. Notably, the combination group showed the most marked increase in p-AMPK levels, suggesting a synergistic enhancement of AMPK activation and its downstream metabolic effects. In terms of insulin levels, the combination group significantly outperformed the Met group; however, no statistical difference was observed compared to the BBR group. This may be due to the fact that BBR alone had already achieved a near-maximal effect in improving insulin resistance, thus limiting the observable benefit of further combination. Furthermore, while we have evaluated the AMPK inhibition in vitro, there is still a lack of in vivo validation. Specific interventions, such as AMPK knockout or pharmacological agonists, would yield clearer proof of this pathway's involvement.

In conclusion, combined metformin and berberine treatment activates AMPK, inhibits SREBP1 and FASN, and suppresses hepatic lipogenesis, thereby ameliorating NAFLD-related steatosis and metabolic dysfunctions. These results validate their therapeutic promise in preclinical animals and clarify the molecular basis of their synergistic actions. This study offers new insights into multi-target approaches for NAFLD treatment, warranting further mechanistic studies, optimization of therapeutic regimens, and clinical evaluation.

## Materials and methods

### Animal experiments and interventions

The Animal Ethics Committee of the Cancer Hospital, which is connected with Shandong First Medical University, approved all animal research in accordance with the *National Regulations for the Management of Laboratory Animals* (Ethical License No. SDTHEC2024007033). One week prior to experimentation, six-week-old male C57BL/6J mice (Beijing SPF Biotechnology Co., Ltd., China) were acclimatized under specific pathogen-free (SPF) conditions (22  $\pm$  2 °C, 55  $\pm$  5% humidity, 12-hour light and 12-hour dark cycle). The mice were subsequently allocated to five distinct categories, each containing six individuals: Group one was the normal control (NC), fed a regular diet; Group two received a high-fat diet (HFD); Group three was on the high-fat diet plus Metformin (Met); Group four was on the high-fat diet plus berberine (BBR); and finally, Group five received a combination of Metformin and berberine (Met + BBR). Except for the NC group, all animals were fed a high-fat diet (D12492, Research Diets Inc., USA) containing 60% fat, 20% protein, and 20% carbohydrate (by energy). The dietary fat mainly originated from lard and soybean oil. After 6 weeks of high-fat diet feeding to induce NAFLD, drug intervention was initiated at week 7 and continued for 12 weeks (i.e., from week 7 to week 18). Metformin (200 mg/kg)<sup>29</sup>, berberine (100 mg/kg)<sup>30</sup>, or both (at the same doses) were dissolved in sterile saline and administered orally once daily by gavage at a volume of 10 mL/kg. The NC and HFD groups received an equivalent volume of sterile saline. As illustrated in Fig. 1a, the experimental procedure included modeling, pharmacological intervention, and sample collection phases.

Upon completion of the treatment phase, after a 12-hour fasting period overnight, the mice were sedated using sodium pentobarbital (administered intraperitoneally at 150 mg/kg). Blood samples were obtained via retro-orbital puncture and then centrifuged to isolate serum. Liver and fat tissues were carefully excised, with portions either flash-frozen in liquid nitrogen for subsequent molecular studies or preserved in 4% paraformaldehyde for tissue examination. This research adheres to the ARRIVE guidelines (available at <https://arriveguidelines.org>) for reporting animal studies.

### Cell culture methods

The HepG2 cell strain, a human liver cancer cell model, was sourced from the reputable China Center for Type Culture Collection (CCTCC). This strain thrives under standard lab conditions: incubated at a balmy 37 °C, surrounded by a cozy atmosphere of 5% CO<sub>2</sub>. For cell upkeep, we've kept them on their toes in high-glucose DMEM from Gibco (the United States), fortifying their regimen with a 10% fetal bovine serum (FBS) addition, also from Gibco, and a pinch of 1% penicillin–streptomycin from Servicebio (China)<sup>31</sup>.

To induce lipid accumulation, cells subjected to 200  $\mu$ M oleic acid and 100  $\mu$ M palmitic acid treatments (in Psaitong, China). Stock solutions (10 mM) were prepared in sodium hydroxide and dispersed in DMEM with added 10% fetal bovine serum (FBS) and 1% BSA to enhance lipid dissolution<sup>32</sup>.

Cells were divided into five groups: Control, OA/PA, OA/PA + Met (2 mM), OA/PA + BBR (1  $\mu$ M), and OA/PA + Met (2 mM) + BBR (1  $\mu$ M). For AMPK inhibition experiments, an additional group was pre-treated with

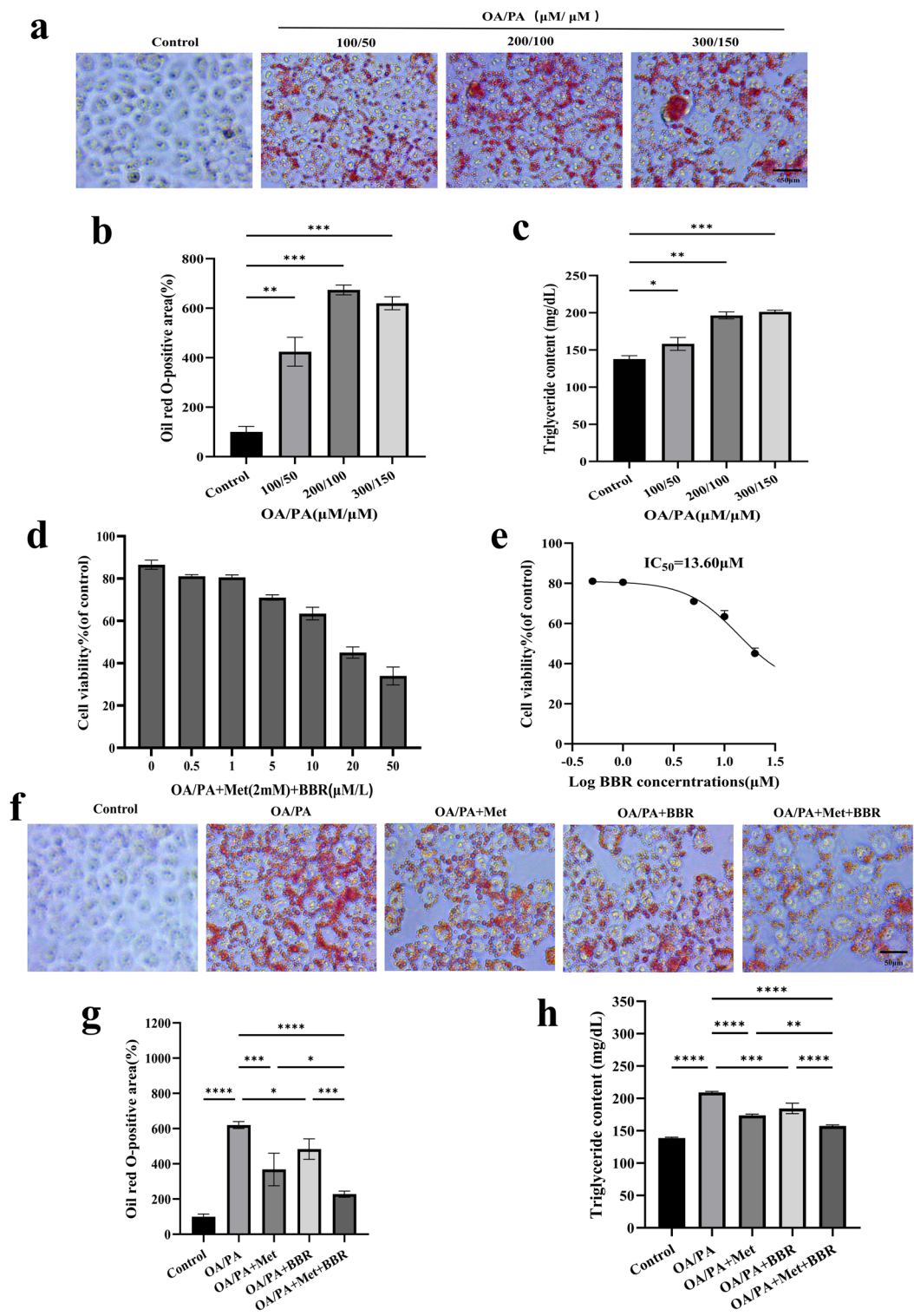


**Fig. 4.** Synergistic reduction of OA/PA-induced lipid accumulation by metformin combined with berberine in HepG2 cells. **(a)** Oil Red O staining images of lipid deposition induced by OA/PA at various concentrations (magnification = 40 $\times$ ; scale bar = 50  $\mu\text{m}$ ); **(b-c)** Quantitative analyses of lipid area and TG content; **(d)** Cell viability assay; **(e)**  $IC_{50}$  determination of drug treatment; **(f-h)** Oil Red O staining, TG content measurement, and image quantification across different treatment groups (magnification = 40 $\times$ ; scale bar = 50  $\mu\text{m}$ ). Data are presented as mean  $\pm$  SEM ( $n = 3$ ). \* $p < 0.05$ , \*\* $p < 0.01$ , \*\*\* $p < 0.001$ , \*\*\*\* $p < 0.0001$ .

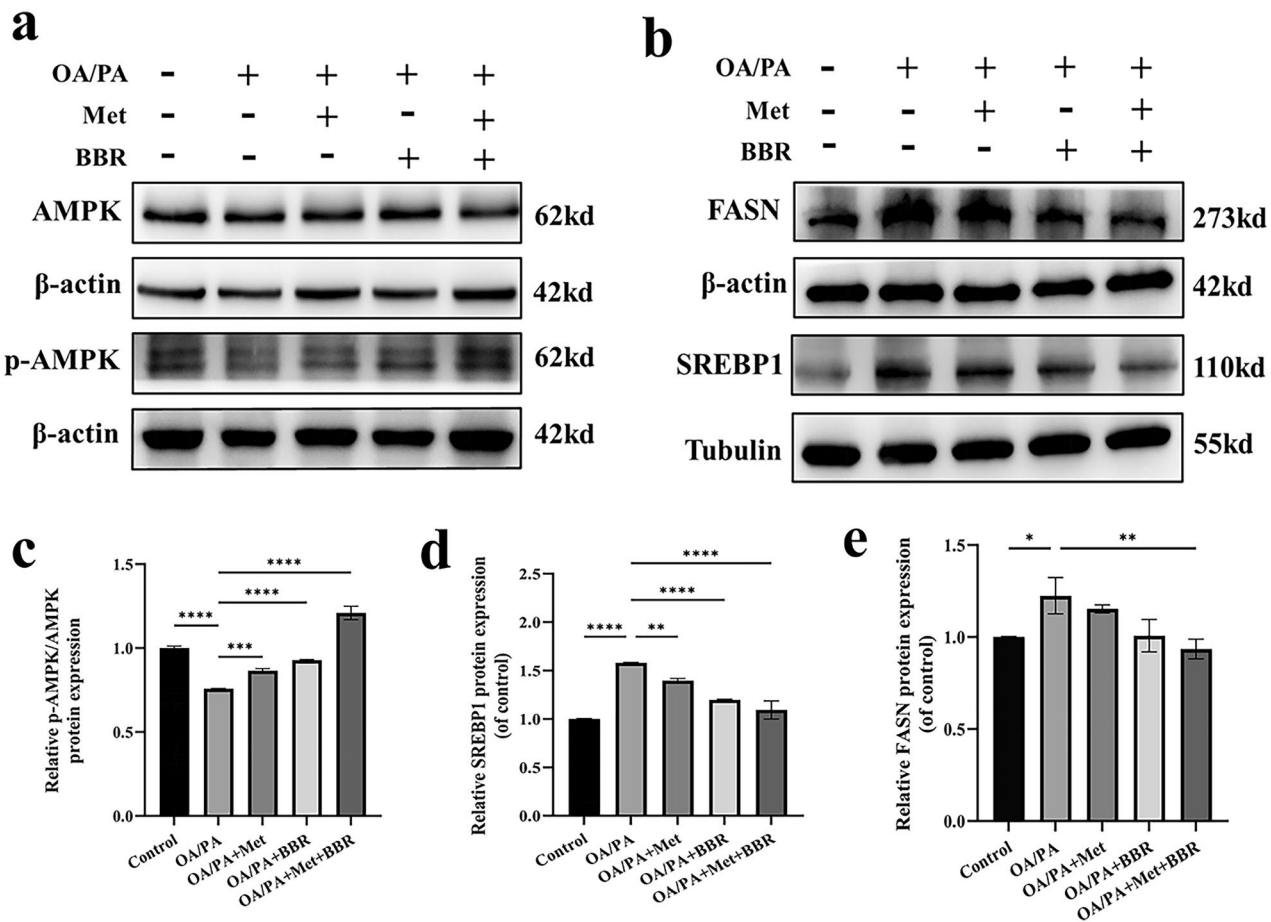


**Fig. 5.** Metformin combined with berberine synergistically activates AMPK and inhibits SREBP1 and FASN expression in HepG2 cells. (a–b) Western blot images of p-AMPK/AMPK, SREBP1 and FASN; (c–e) Densitometric analyses of protein expression levels. To highlight the target bands, the images were cropped; the full-length gel/blot images are provided in the Supplementary Material. Data are presented as mean  $\pm$  SEM ( $n=3$ ). \*\*\* $p<0.001$ , \*\*\*\* $p<0.0001$ .

Compound C (10  $\mu$ M; Selleck, China) for 1 h prior to OA/PA exposure. All treatments were completed within 24 h. Metformin and BBR concentrations (2 mM and 1  $\mu$ M, respectively) were selected based on preliminary cell viability assays (MTT) (Fig. 4d–e).

#### Assessment of cell viability using the MTT assay

To gauge cellular viability, the MTT method was deployed. HepG2 cells were sown into 96-well plates at a concentration of  $5 \times 10^4$  cells per mL. Following a 24-hour treatment period, a 20- $\mu$ L dose of MTT solution (5 mg/mL, sourced from Solarbio, China) was introduced to each well, which was then incubated for a spell at 37 °C. Following this, the solvent was subjected to aspiration, and then 150  $\mu$ L of DMSO from Solarbio (China) was added to dissolve the formazan salts. The relative cell viability was assessed by measuring the absorbance at 570 nm with a microplate reader.

#### Biochemical parameter detection

Blood samples were analyzed for ALT, AST, total cholesterol (TC), triglycerides (TG), HDL cholesterol (HDL-C), and LDL cholesterol (LDL-C) using standardized automated biochemical testing equipment. GLU was obtained with a Swiss-made Accu-Chek Performa glucose monitor, while INS concentrations were quantified through ELISA testing using kits from Elabscience. Insulin resistance was evaluated using the standard HOMA-IR calculation. Liver tissue cholesterol and triglyceride levels were assessed with Solarbio test kits, and intracellular TG accumulation in HepG2 cells was measured using Psaitong diagnostic kits, with all procedures following the manufacturers' established protocols.

#### Histological staining and NAFLD activity scoring

Liver specimens were processed by paraffin embedding, 4% paraformaldehyde fixation, and 5  $\mu$ m sectioning. Subsequent to dehydration and rehydration, H&E staining was applied. Following embedding in OCT compound, fresh liver tissues were frozen-sectioned to 10  $\mu$ m at -20 °C followed by 0.5% Oil Red O staining. Hematoxylin was used as a counterstain. The HepG2 cell samples were preserved using a 4% paraformaldehyde

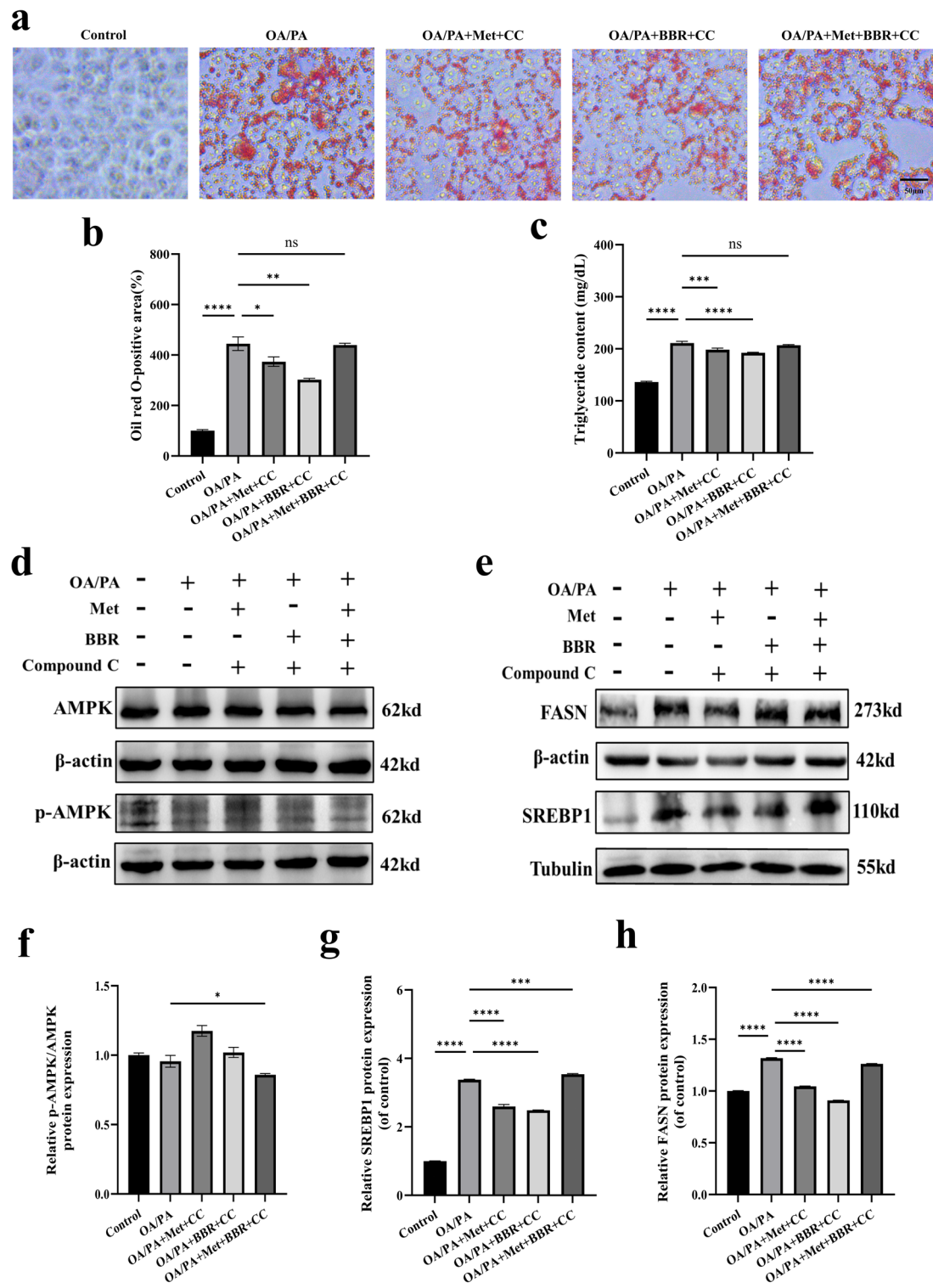


**Fig. 6.** Metformin combined with berberine inhibits lipid synthesis through the AMPK–SREBP1–FASN signaling pathway. (a) Oil Red O staining images after AMPK inhibitor treatment (magnification = 40 $\times$ ; scale bar = 50  $\mu$ m); (b–c) Quantitative analysis of intracellular Oil Red O staining and triglyceride (TG) content. (d–e) Western blot showing expression changes of p-AMPK, SREBP1 and FASN proteins; (f–h) Quantitative analyses of protein grayscale values. To highlight the target bands, the images were cropped; the full-length gel/blot images are provided in the Supplementary Material. Data are presented as mean  $\pm$  SEM ( $n=3$ ). \* $p < 0.05$ , \*\* $p < 0.01$ , \*\*\* $p < 0.001$ , \*\*\*\* $p < 0.0001$ , ns: not significant.

solution, thoroughly rinsed with phosphate-buffered saline (PBS), and then treated with a 0.5% Oil Red O stain for half an hour. Both the stained liver tissue sections and cellular samples were examined under a Nikon light microscope, with subsequent image processing and analysis performed through ImageJ software. The state of cell oil red O staining was photographed by Zeiss Axio Vert.A1 inverted microscope, observed using 20 $\times$  objective lens, uniformly stored in TIFF format, without image post-processing.

The NAS was used to evaluate liver histopathology, including steatosis (0–3), lobular inflammation (0–2), and ballooning degeneration (0–2). A NAS of  $\geq 5$  was considered diagnostic of non-alcoholic steatohepatitis (NASH), while a score of  $< 3$  was defined as non-NASH.

### Analysis via Western blot techniques

Liver tissues and HepG2 cells were processed using RIPA lysis buffer to extract proteins, which were then measured for concentration via the BCA method employing the Beyotime kit (China). Equal protein aliquots (30  $\mu$ g) underwent SDS-PAGE separation and subsequent transfer onto PVDF membranes (Merck, China). The study utilized these primary antibodies:  $\beta$ -actin, sourced from Bioss in China (cat. no. bs-0061R), prepared at a 1:5000 dilution; Tubulin, obtained from UpingBio, China (cat. no. YP-Ab-10638), with a 1:1000 dilution ratio; total AMPK alpha from Cell Signaling Technology in the USA (cat. no. 5831), also diluted at 1:1000; phospho-AMPK alpha from the same source (cat. no. 2535), again at 1:1000; FASN, supplied by Cell Signaling Technology, USA (cat. no. 3180), diluted 1:1000; and SREBP1, from UpingBio, China (cat. no. YP-mAb-10754), prepared to a 1:1000 concentration. All antibodies were rabbit polyclonal except for the SREBP1 antibody, which was mouse monoclonal. Once cleaned, the samples were exposed to HRP-linked secondary antibodies for a full hour at normal temperature. The protein patterns were then made visible through the use of the Biosharp ECL reagent from China and were measured with the help of ImageJ software. We hereby declare that our Western blot data fully comply with digital image processing and data integrity guidelines. The uncropped original blot images corresponding to Figs. 3h and i, 5a-b and 6d-e are provided in the Supplementary Figures.

### Statistical analysis

Results are reported as means  $\pm$  standard error of the mean (SEM). Data analysis was conducted in GraphPad Prism, employing either one-way ANOVA or two-tailed Student's t-tests depending on experimental design. A p-value of less than 0.05 was considered statistically significant for all comparisons.

### Data availability

The datasets generated and/or analyzed in this study are available from the corresponding author upon reasonable request.

Received: 10 June 2025; Accepted: 7 August 2025

Published online: 11 August 2025

### References

1. Koperska, A., Wesolek, A., Moszak, M. & Szulinska, M. Berberine in Non-Alcoholic fatty liver Disease—A review. *Nutrients* **14**, 3459 (2022).
2. Santhekadur, P. K., Kumar, D. P. & Sanyal, A. J. Preclinical models of non-alcoholic fatty liver disease. *J. Hepatol.* **68**, 230–237 (2018).
3. Ratziu, V. Starting the battle to control non-alcoholic steatohepatitis. *Lancet* **385**, 922–924 (2015).
4. Cheng, D. et al. Metformin attenuates silica-induced pulmonary fibrosis via AMPK signaling. *J. Transl Med.* **19**, 349 (2021).
5. Ma, T. et al. Low-dose Metformin targets the lysosomal AMPK pathway through PEN2. *Nature* **603**, 159–165 (2022).
6. Song, D., Hao, J. & Fan, D. Biological properties and clinical applications of Berberine. *Front. Med.* **14**, 564–582 (2020).
7. Brusq, J. M. et al. Inhibition of lipid synthesis through activation of AMP kinase: an additional mechanism for the hypolipidemic effects of Berberine. *J. Lipid Res.* **47**, 1281–1288 (2006).
8. Rena, G., Hardie, D. G. & Pearson, E. R. The mechanisms of action of Metformin. *Diabetologia* **60**, 1577–1585 (2017).
9. Kim, T. S. et al. Metformin and Dichloroacetate suppress proliferation of liver cancer cells by inhibiting mTOR complex 1. *Int. J. Mol. Sci.* **22**, 10027 (2021).
10. Madiraju, A. K. et al. Metformin suppresses gluconeogenesis by inhibiting mitochondrial glycerophosphate dehydrogenase. *Nature* **510**, 542–546 (2014).
11. Xu, X. et al. Berberine alleviates nonalcoholic fatty liver induced by a high-fat diet in mice by activating SIRT3. *FASEB J.* **33**, 7289–7300 (2019).
12. Yu, M. et al. Berberine alleviates lipid metabolism disorders via Inhibition of mitochondrial complex I in gut and liver. *Int. J. Biol. Sci.* **17**, 1693–1707 (2021).
13. Zhu, X. et al. Combination of Berberine with Resveratrol improves the Lipid-Lowering efficacy. *Int. J. Mol. Sci.* **19**, 3903 (2018).
14. Qin, G. et al. Isoquercetin improves hepatic lipid accumulation by activating AMPK pathway and suppressing TGF- $\beta$  signaling on an HFD-Induced nonalcoholic fatty liver disease rat model. *Int. J. Mol. Sci.* **19**, 4126 (2018).
15. Zamani-Garmsiri, F. et al. Combination of Metformin and genistein alleviates non-alcoholic fatty liver disease in high-fat diet-fed mice. *J. Nutr. Biochem.* **87**, 108505 (2021).
16. Ramadan, N. M., Elmasry, K., Elsayed, H. R. H., El-Mesery, A. & Eraky, S. M. The hepatoprotective effects of n3-polyunsaturated fatty acids against non-alcoholic fatty liver disease in diabetic rats through the FOXO1/PPAR $\alpha$ /GABARAPL1 signalling pathway. *Life Sci.* **311**, 121145 (2022).
17. Tehrani, S. S., Goodarzi, G., Panahi, G., Zamani-Garmsiri, F. & Meshkani, R. The combination of Metformin with Morin alleviates hepatic steatosis via modulating hepatic lipid metabolism, hepatic inflammation, brown adipose tissue thermogenesis, and white adipose tissue Browning in high-fat diet-fed mice. *Life Sci.* **323**, 121706 (2023).
18. Diniz, T. A. et al. Aerobic training improves NAFLD markers and insulin resistance through AMPK-PPAR $\alpha$  signaling in obese mice. *Life Sci.* **266**, 118868 (2021).
19. Smith, B. K. et al. Treatment of nonalcoholic fatty liver disease: role of AMPK. *Am. J. Physiol. Endocrinol. Metab.* **311**, E730–E740 (2016).
20. O'Farrell, M. et al. FASN Inhibition targets multiple drivers of NASH by reducing steatosis, inflammation and fibrosis in preclinical models. *Sci. Rep.* **12**, 15661 (2022).

21. Garcia, D. et al. Genetic Liver-Specific AMPK activation protects against Diet-Induced obesity and NAFLD. *Cell. Rep.* **26**, 192–208e6 (2019).
22. Herzig, S. & Shaw, R. J. AMPK: guardian of metabolism and mitochondrial homeostasis. *Nat. Rev. Mol. Cell. Biol.* **19**, 121–135 (2018).
23. Xu, X., So, J. S., Park, J. G. & Lee, A. H. Transcriptional control of hepatic lipid metabolism by SREBP and ChREBP. *Semin Liver Dis.* **33**, 301–311 (2013).
24. Li, Y. et al. AMPK phosphorylates and inhibits SREBP activity to attenuate hepatic steatosis and atherosclerosis in Diet-induced insulin resistant mice. *Cell. Metab.* **13**, 376–388 (2011).
25. Sapp, V., Gaffney, L., EauClaire, S. F. & Matthews, R. P. Fructose leads to hepatic steatosis in zebrafish that is reversed by mechanistic target of Rapamycin (mTOR) Inhibition. *Hepatology* **60**, 1581–1592 (2014).
26. Sangüesa, G. et al. mTOR is a key protein involved in the metabolic effects of simple sugars. *Int. J. Mol. Sci.* **20**, 1117 (2019).
27. Pawlak, M., Lefebvre, P. & Staels, B. Molecular mechanism of PPAR $\alpha$  action and its impact on lipid metabolism, inflammation and fibrosis in non-alcoholic fatty liver disease. *J. Hepatol.* **62**, 720–733 (2015).
28. Guo, T. et al. Berberine ameliorates hepatic steatosis and suppresses liver and adipose tissue inflammation in mice with Diet-induced obesity. *Sci. Rep.* **6**, 22612 (2016).
29. Finisguerra, V. et al. Metformin improves cancer immunotherapy by directly rescuing tumor-infiltrating CD8 T lymphocytes from hypoxia-induced immunosuppression. *J. Immunother. Cancer.* **11**, e005719 (2023).
30. Wang, Z. et al. Berberine improves ovulation and endometrial receptivity in polycystic ovary syndrome. *Phytomedicine* **91**, 153654 (2021).
31. Rafiei, H., Omidian, K. & Bandy, B. Dietary polyphenols protect against oleic Acid-Induced steatosis in an in vitro model of NAFLD by modulating lipid metabolism and improving mitochondrial function. *Nutrients* **11**, 541 (2019).
32. Gómez-Lechón, M. J. et al. A human hepatocellular in vitro model to investigate steatosis. *Chem. Biol. Interact.* **165**, 106–116 (2007).

## Acknowledgements

This research was funded by grants from the National Natural Science Foundation of China (Award No. 8227071910), the Shandong Provincial Natural Science Foundation (Award No. ZR2021MH060), and the Beijing Medical Development Foundation for Science and Technology Innovation (Award No. KC2023-JX-0288-FZ125).

## Author contributions

By conducting experiments and writing the manuscript, N. L. and Q.C. made equal contributions to this study and share first authorship; X.G. was in charge of interpreting and analyzing the data; Fang Liu edited and made major revisions to the work. Contributions to the experimental work came from B.Z.; Q.W. and H.Z.; JJ Han secured funding, designed and supervised the study, and revised the manuscript. The final draft of the manuscript has been read and approved by all writers.

## Funding

Support for this effort came from the National Natural Science Foundation of China (Grant No.8227071910), the Natural Science Foundation of Shandong Province (Grant No. ZR2021MH060), and the Beijing Science and Technology Innovation Medical Development Foundation Research Fund Project (Grant No. KC2023-JX-0288-FZ125). The research's methodology, data acquisition, examination, and conclusions, together with the manuscript composition, were conducted without influence from the sponsors.

## Declarations

### Competing interests

The authors declare no competing interests.

### Ethical compliance

This research was conducted in strict accordance with the “National Standards for Laboratory Animal Care and Use” and adhered to the ethical guidelines established by the Animal Experiment Ethics Committee of Shandong First Medical University Affiliated Cancer Hospital. The study received formal ethical approval (Approval No.: SDTHEC2024007033) to ensure all procedures met institutional and regulatory requirements.

### Additional information

**Supplementary Information** The online version contains supplementary material available at <https://doi.org/10.1038/s41598-025-15495-7>.

**Correspondence** and requests for materials should be addressed to J.-J.H.

**Reprints and permissions information** is available at [www.nature.com/reprints](http://www.nature.com/reprints).

**Publisher's note** Springer Nature remains neutral with regard to jurisdictional claims in published maps and institutional affiliations.

**Open Access** This article is licensed under a Creative Commons Attribution-NonCommercial-NoDerivatives 4.0 International License, which permits any non-commercial use, sharing, distribution and reproduction in any medium or format, as long as you give appropriate credit to the original author(s) and the source, provide a link to the Creative Commons licence, and indicate if you modified the licensed material. You do not have permission under this licence to share adapted material derived from this article or parts of it. The images or other third party material in this article are included in the article's Creative Commons licence, unless indicated otherwise in a credit line to the material. If material is not included in the article's Creative Commons licence and your intended use is not permitted by statutory regulation or exceeds the permitted use, you will need to obtain permission directly from the copyright holder. To view a copy of this licence, visit <http://creativecommons.org/licenses/by-nc-nd/4.0/>.

© The Author(s) 2025